



Supporting Information

for

The reaction of arylmethyl isocyanides and arylmethylamines with xanthate esters: a facile and unexpected synthesis of carbamothioates

Narasimhamurthy Rajeev, Toreshettahally R. Swaroop, Ahmad I. Alrawashdeh, Shofiur Rahman, Abdullah Alodhayb, Seegehalli M. Anil, Kuppalli R. Kiran, Chandra, Paris E. Georghiou, Kanchugarakoppal S. Rangappa and Maralinganadoddi P. Sadashiva

Beilstein J. Org. Chem. **2020**, *16*, 159–167. [doi:10.3762/bjoc.16.18](https://doi.org/10.3762/bjoc.16.18)

Experimental procedures, analytical data, copies of ^1H and ^{13}C NMR spectra of all studied compounds, and computational details

Table of Contents

	<u>Page</u>
Experimental Section	S2
Table 1: Crystal data and structure refinement for 4c	S6
Table 2: Bond lengths [Å] and angles [°] for 4c	S7
Figure S1: ¹ H and ¹³ C NMR spectra of 4a	S8
Figure S2: ¹ H and ¹³ C NMR spectra of 4b	S9
Figure S3: ¹ H and ¹³ C NMR spectra of 4c	S10
Figure S4: ¹ H and ¹³ C NMR spectra of 4d	S11
Figure S5: ¹ H and ¹³ C NMR spectra of 4e	S12
Figure S6: ¹ H and ¹³ C NMR spectra of 4f	S13
Figure S7: ¹ H and ¹³ C NMR spectra of 4g	S14
Figure S8: ¹ H and ¹³ C NMR spectra of 4h	S15
Figure S9: ¹ H and ¹³ C NMR spectra of 4i	S16
Figure S10: ¹ H and ¹³ C NMR spectra of 4j	S17
Figure S11: ¹ H and ¹³ C NMR spectra of 4k	S18
Figure S12: ¹ H and ¹³ C NMR spectra of 4l	S19
Figure S13: ¹ H spectra of 4c in DMSO- <i>d</i> ₆ after heating to 60 °C	S20
Figure S14: Total energies (hartrees) along the intrinsic reaction coordinates (IRC)	S21
Table S3: Relative electronic energies (<i>E</i> _{ele}), thermal energies (<i>E</i> _{thermal})	S21
Scheme S1: The alternative mechanism previously considered	S22
Figure S15: The optimized geometries	S23
Figure S16: Relative energies (<i>E</i> _a ; kJ/mol) for the alternative mechanism	S24
References	S24

1. Experimental Section

1.1. General information. The starting materials were purchased from commercial sources. The solvents were of analytical grade and were used without further purification. Reactions were monitored by thin-layer chromatography (TLC) using precoated sheets of silica gel 60 (Merck 60 F₂₅₄, 0.25 mm thickness) and visualization under UV light. The melting points were determined on a SELACO melting point apparatus and are uncorrected. ¹H NMR (400 MHz) and ¹³C NMR (100 MHz) spectra were obtained using an Agilent NMR spectrometer. Chemical shifts (δ) are given in parts per million (ppm) using the residue solvent (CDCl₃) peak as reference relative to TMS. Coupling constant (*J*) values are given in Hz. Mass spectral analysis was performed using a Waters Synapt G2 mass spectrometer. Infrared spectra were recorded on a Shimadzu FT-IR model 8300 spectrophotometer. The X-ray diffraction data were collected on a Bruker SMART APEX II X-ray diffractometer with graphite monochromated MoK α radiation. Raw data was processed and reduced by using APEX2 and SAINT. [SI1] The structure was solved by direct methods and full matrix least squares refinement was carried out using SHELXS-97/SHELXL-97, respectively [SI2]. Geometry optimization and molecular energies were calculated by using B3LYP/ 6-311 ++G(d,p) basis set [SI3].

1.2. General procedure for the synthesis of thionocarbamates:

Method A: To a suspension of sodium hydride (2.0 mmol) in DMF (2.0 mL), a mixture of xanthate ester **1** (1.0 mmol) and arylmethyl isocyanide **2** (1.0 mmol) in DMF (2.0 mL) was added at 0 °C. The stirring was continued for 15 to 30 min (monitored by TLC) at 35 to 45°C. After the completion of the reaction, the reaction mixture was quenched by adding ice cold water (25 mL), extracted with ethyl acetate (2 × 25 mL). The combined organic layer was washed with water (25 mL), brine (25 mL), dried over anhydrous sodium sulfate and concentrated under reduced pressure to get crude products, which were purified by column chromatography over silica gel using 10% ethyl acetate in hexane.

Method B: To a suspension of sodium hydride (2.0 mmol) in DMF (2.0 mL) at 0 °C, a mixture of xanthate ester **1** (1.0 mmol) and arylmethylamine **5** (1.0 mmol) in DMF (2.0 mL) was added and stirred for 1 to 1.5 h (monitored by TLC) at 35 to 45°C. After the completion of reaction, the reaction mixture was quenched by adding ice cold water (25 mL), extracted with ethyl acetate (2 × 25 mL). The combined organic layer was washed with water (25 mL), brine (25 mL), dried over anhydrous sodium sulphate and concentrated under

reduced pressure to get crude products, which were purified by column chromatography over silica gel using 10% ethyl acetate in hexane. The yields from Method B are shown in parentheses.

O-benzyl benzylcarbamothioate (**4a**). Colourless solid (mp 52-54 °C). 85%, 220 mg (80%, 210 mg). Rotamers ratio 66:34. IR (KBr, cm⁻¹) ν 636, 1069, 1285, 1328, 2936, 3256. ¹H NMR (CDCl₃, 400 MHz, δ) 4.44 (d, J = 6.0 Hz, 2H, CH₂), 4.76 (d, J = 5.6 Hz, 2H, CH₂), 5.51 (s, 2H, CH₂), 5.55 (s, 2H, CH₂), 6.58 (s, 1H, NH), 7.0 (s, 1H, NH), 7.19-7.39 (m, 20H, Ar-H). ¹³C NMR (CDCl₃, 100 MHz, δ) 190.3, 189.7, 136.7, 135.7, 128.8, 128.8, 128.7, 128.5, 128.5, 128.4, 128.3, 128.2, 127.9, 127.9, 127.7, 127.6, 127.2, 73.3, 72.1, 49.4, 47.3 (1 peak lost). HRMS (ESI) [M+H]⁺ Anal. Calcd for C₁₅H₁₆NOS: 258.0953; Found: 258.0957.

O-benzyl (4-methylbenzyl)carbamothioate (**4b**). Colourless solid (mp 60-62°C). 84%, 230 mg (82%, 220 mg). Rotamers ratio 64:36. IR (KBr, cm⁻¹) ν 626, 1055, 1274, 1326, 2920, 3197. ¹H NMR (CDCl₃, 400 MHz, δ) 2.33 (s, 6H, 2CH₃), 4.42 (d, J = 5.2 Hz, 2H, CH₂), 4.71 (d, J = 5.2 Hz, 2H, CH₂), 5.49 (s, 2H, CH₂), 5.55 (s, 2H, CH₂), 7.11-7.37 (m, 18H, Ar-H). ¹³C NMR (CDCl₃, 100 MHz, δ) 190.0, 189.3, 137.4, 129.4, 129.4, 128.8, 128.5, 128.5, 128.3, 128.3, 128.1, 127.9, 127.7, 127.1, 72.0, 71.1, 47.2, 45.2, 29.6, 21.0 (4 peaks lost). HRMS (ESI) [M+H]⁺ Anal. Calcd for C₁₆H₁₈NOS: 272.1109; Found: 272.1104.

O-benzyl (4-fluorobenzyl)carbamothioate (**4c**). Yellow solid (mp 72-75°C). 87%, 240 mg (77%, 210 mg). Rotamers ratio 65:35. IR (KBr, cm⁻¹) ν 634, 1056, 1265, 1326, 2920, 3256. ¹H NMR (CDCl₃, 400 MHz, δ) 4.42 (d, J = 6.0 Hz, 2H, CH₂), 4.73 (d, J = 5.6 Hz, 2H, CH₂), 5.49 (s, 2H, CH₂), 5.53 (s, 2H, CH₂), 6.52 (s, 1H, NH), 6.96 (s, 1H, NH), 6.97-7.05 (m, 4H, Ar-H), 7.14-7.18 (t, J = 5.2 Hz, 1H, ArH), 7.21-7.25 (m, 1H, Ar-H), 7.27-7.38 (m, 12H, Ar-H). ¹³C NMR (CDCl₃, 100 MHz, δ) 190.4, 189.6, 163.6 (J = 34.0 Hz), 161.1 (J = 34.0 Hz), 135.6, 132.5, 129.7, 129.6, 129.4, 129.3, 128.8, 128.6, 128.4, 128.3, 127.2, 115.7, 115.5, 115.4, 73.4, 72.2, 48.6, 46.6. HRMS (ESI) [M+H]⁺ Anal. Calcd for C₁₅H₁₅FNOS: 276.0858; Found: 276.0851.

O-(2-methylbenzyl) benzylcarbamothioate (**4d**). Viscous liquid. 81%, 220 mg (81%, 220 mg). Rotamers ratio 66:34. IR (KBr, cm⁻¹) ν 696, 1056, 1323, 1596, 2865, 3206. ¹H NMR (CDCl₃, 400 MHz, δ) 2.28 (s, 3H, Ar-CH₃), 2.36 (s, 3H, Ar-CH₃), 4.41 (d, J = 6.4 Hz, 2H, Ar-CH₂), 4.76 (d, J = 5.6 Hz, 2H, Ar-CH₂), 5.50-5.53 (two singlet, 4H, 2CH₂), 7.15-7.36 (m, 18H, Ar-H). ¹³C NMR (CDCl₃, 100 MHz, δ) 190.9, 190.2, 138.9, 138.6, 136.9, 136.7, 136.9, 133.9, 133.5, 130.3, 130.3, 129.6, 129.5, 128.7, 128.0, 127.9, 127.6, 126.0, 125.9, 72.0, 70.7, 49.2, 47.3, 18.9, 18.8 (3 peaks lost). HRMS (ESI) [M+H]⁺ Anal. Calcd for C₁₆H₁₈NOS: 272.1109; Found: 272.1105.

O-(3-methoxybenzyl) (4-fluorobenzyl)carbamothioate (**4e**). Colourless solid (mp 74-76°C). 83%, 250 mg (75%, 230 mg). Rotamers ratio 100:0. IR (KBr, cm⁻¹) ν 690, 1097, 1353, 1482, 1584, 2852, 3015. ¹H NMR (CDCl₃, 400 MHz, δ) 3.77 (s, 3H, OCH₃), 4.15 (s, 2H, CH₂), 4.43 (d, J = 5.6 Hz, 2H, CH₂), 5.61 (s, 1H, NH), 6.78 (dd, J = 8.2 Hz, 2.4 Hz, 1H, Ar-H), 6.88-6.92 (m, 2H, Ar-H), 7.00 (t, J = 8.4 Hz, 2H, Ar-H), 7.18-7.25 (m, 3H, Ar-H). ¹³C NMR (CDCl₃, 100 MHz, δ) 190.1, 163.5 (J =31.0 Hz), 159.7, 139.6, 129.5, 129.4, 121.1, 115.6, 115.5, 114.3, 112.9, 55.1, 44.7, 34.3. HRMS (ESI) [M+H]⁺ Anal. Calcd for C₁₆H₁₇FNO₂S: 306.0964; Found: 306.0969.

O-(3-methoxybenzyl) (4-chlorobenzyl)carbamothioate (**4f**). Viscous liquid. 79%, 250 mg (83%, 270 mg). Rotamers ratio 100:0. IR (KBr, cm⁻¹) ν 692, 1040, 1318, 1486, 1593, 2920, 3025. ¹H NMR (CDCl₃, 400 MHz, δ) 3.80 (s, 3H, OCH₃), 4.15 (s, 2H, CH₂), 4.43 (d, J = 5.6 Hz, 2H, CH₂), 5.64 (s, 1H, NH), 6.76-6.79 (m, 1H, Ar-H), 6.89-7.17 (m, 2H, Ar-H), 7.18-7.29 (m, 5H, Ar-H). ¹³C NMR (CDCl₃, 100M Hz, δ) 190.1, 159.7, 138.3, 137.3, 136.3, 129.5, 128.9, 128.8, 121.0, 114.2, 112.9, 55.1, 34.3, 29.6. HRMS (ESI) [M+H]⁺ Anal. Calcd for C₁₆H₁₇ClNO₂S: 322.0669; Found: 322.0661.

O-(4-bromobenzyl) benzylcarbamothioate (**4g**). Yellow solid (mp 110-115°C). 80%, 270 mg (82%, 270 mg). Rotamers ratio 56:44. IR (KBr, cm⁻¹) ν 746, 1041, 1294, 1593, 2920, 3204. ¹H NMR (CDCl₃, 400 MHz, δ) 4.43 (d, J = 6.0 Hz, 2H, CH₂), 4.75 (d, J = 5.6 Hz, 2H, CH₂), 5.45-5.48 (two singlet, 4H, 2CH₂), 6.6 (s, 1H, NH), 7.00 (s, 1H, NH), 7.16-7.34 (m, 16H, Ar-H), 7.35-7.48 (m, 2H, Ar-H). ¹³C NMR (CDCl₃, 100 MHz, δ) 190.5, 190.0, 136.5, 134.8, 131.6, 131.6, 130.6, 130.5, 130.0, 129.8, 128.8, 128.8, 128.0, 128.0, 127.5, 72.3, 71.0, 49.5, 47.4 (3 peaks lost). HRMS (ESI) [M+H]⁺ Anal. Calcd for C₁₅H₁₅BrNOS: 336.0058 and 338.0037; Found: 336.0051 and 338.0032.

O-(4-bromobenzyl) (4-methylbenzyl)carbamothioate (**4h**). Yellow solid (mp 96-98 °C). 76%, 260 mg (86%, 300 mg). Rotamers ratio 58:42. IR (KBr, cm⁻¹) ν 747, 1061, 1285, 1549, 2923, 3225. ¹H NMR (CDCl₃, 400 MHz, δ) 2.31 & 2.33 (two singlet, 6H, 2CH₃), 4.39 (d, J = 5.6 Hz, 2H, CH₂), 4.70 (d, J = 5.2 Hz, 2H, CH₂), 5.44 & 5.49 (s, 2H, CH₂), 6.5 (s, 1H, NH), 6.9 (s, 1H, NH), 7.07-7.25 (m, 14H, Ar-H), 7.39-7.48 (m, 2H, Ar-H). ¹³C NMR (CDCl₃, 100 MHz, δ) 190.7, 189.8, 137.7, 134.8, 133.5, 131.6, 131.6, 130.5, 129.9, 129.8, 129.4, 129.2, 128.0, 127.9, 127.5, 122.3, 72.3, 70.9, 49.3, 47.1, 29.6, 21.0 (2 peaks lost). HRMS (ESI) [M+H]⁺ Anal. Calcd for C₁₆H₁₇BrNOS: 350.0214 and 352.0194; Found: 350.0219 and 352.0198.

O-butyl (4-fluorobenzyl)carbamothioate (**4i**). Viscous liquid. 86%, 210 mg (74%, 180 mg). Rotamers ratio 60:40. IR (KBr, cm^{-1}) ν 626, 1057, 1323, 1584, 1695, 3076, 3235. ^1H NMR (CDCl_3 , 400 MHz, δ) 0.83-0.94 (m, 6H, 2 CH_3), 1.24-1.43 (m, 4H, 2 CH_2), 1.62-1.71 (m, 4H, 2 CH_2), 4.49-4.69 (m, 4H, 2 CH_2), 4.71 (d, $J = 6.0$ Hz, 4H, 2 CH_2), 6.43 (s, 1H, NH), 6.98-7.03 (m, 4H, Ar-H), 7.19-7.30 (m, 4H, Ar-H). ^{13}C NMR (CDCl_3 , 100 MHz, δ) 190.9, 190.1, 163.6 ($J=28.0$ Hz), 161.1 ($J=28.0$ Hz), 129.7, 129.6, 129.3, 129.2, 115.8, 115.7, 115.6, 115.5, 72.0, 70.6, 48.4, 46.4, 30.7, 30.6, 19.0, 13.7, 13.6. HRMS (ESI) $[\text{M}+\text{H}]^+$ Anal. Calcd for $\text{C}_{12}\text{H}_{17}\text{FNOS}$: 242.1015; Found: 242.1019.

O-butyl (4-chlorobenzyl)carbamothioate (**4j**). Viscous liquid. 84%, 220 mg (79%, 200 mg). Rotamers ratio 62:38. IR (KBr, cm^{-1}) ν 632, 1054, 1307, 1584, 3074, 3224. ^1H NMR (CDCl_3 , 400 MHz, δ) 0.89-1.24 (m, 6H, 2 CH_3), 1.27-1.41 (m, 4H, 2 CH_2), 1.56-1.70 (m, 4H, 2 CH_2), 4.38-4.71 (m, 4H, 2 CH_2), 4.72 (d, $J = 5.6$ Hz, 2H, CH_2), 6.4 (s, 1H, NH), 6.8 (s, 1H, NH), 7.15-7.31 (m, 8H, Ar-H). ^{13}C NMR (CDCl_3 , 100 MHz, δ) 190.8, 190.0, 137.2, 135.4, 129.1, 128.9, 128.8, 128.7, 127.9, 127.1, 72.1, 70.7, 48.3, 48.4, 30.6, 30.5, 29.6, 19.0, 13.7, 13.6 (2 peaks lost). HRMS (ESI) $[\text{M}+\text{H}]^+$ Anal. Calcd for $\text{C}_{12}\text{H}_{17}\text{ClNOS}$: 258.0719; Found: 258.0711.

O-(3-methylcyclohexyl) benzylcarbamothioate (**4k**). Viscous liquid. 82%, 220 mg (81%, 210 mg). Rotamers ratio 57:43. IR (KBr, cm^{-1}) ν 626, 1318, 1236, 1523, 2896, 3221. ^1H NMR (CDCl_3 , 400 MHz, δ) 0.79-1.05 (m, 12H, 2CH, 2 CH_2 , 2 CH_3), 1.17-1.63 (m, 4H, 2 CH_2), 1.75-1.78 (m, 1H, CH), 2.09-2.12 (m, 4H, 2 CH_2), 4.4 (d, $J = 6.0$ Hz, 2H, CH_2), 4.73 (d, $J = 5.60$ Hz, 2H, CH_2), 5.23-5.29 (m, 2H, CH), 6.37 (s, 1H, NH), 7.0 (s, 1H, NH), 7.21-7.34 (m, 10H, Ar-H). ^{13}C NMR (CDCl_3 , 100 MHz, δ) 190.2, 189.5, 136.9, 128.7, 128.7, 127.9, 127.8, 127.7, 127.6, 81.2, 79.3, 49.1, 47.0, 40.4, 40.2, 34.0, 33.9, 31.4, 31.3, 31.2, 31.2, 23.8, 23.7, 22.2, 22.2 (1 peak lost). HRMS (ESI) $[\text{M}+\text{H}]^+$ Anal. Calcd for $\text{C}_{15}\text{H}_{22}\text{NOS}$: 264.1422; Found: 264.1429.

O-(3-methylcyclohexyl) (4-fluorobenzyl)carbamothioate (**4l**). Viscous liquid. 88%, 250 mg (71%, 200 mg). Rotamers ratio 58:42. IR (KBr, cm^{-1}) ν 638, 1222, 1391, 1508, 2931, 3234. ^1H NMR (CDCl_3 , 400 MHz, δ) 0.76-1.03 (m, 10H, 2 CH_2 , 2 CH_3), 1.16-1.78 (m, 6H, 3 CH_2), 1.89-1.96 (m, 1H, CH), 2.08-2.15 (m, 2H, CH_2), 4.35 (d, $J = 6.0$ Hz, 1H, CH), 4.69 (d, 4H, $J = 5.24$ Hz, 2 CH_2), 5.20-5.29 (m, 2H, 2CH), 5.61 (s, 1H, NH), 6.37 (s, 1H, NH), 6.98-7.04 (m, 4H, Ar-H), 7.18-7.21 (m, 2H, Ar-H), 7.22-7.31 (m, 2H, Ar-H). ^{13}C NMR (CDCl_3 , 100 MHz, δ) 189.9, 189.1, 132.8 ($J=29.0$ Hz), 129.7 ($J=29.0$ Hz), 129.6, 129.4, 129.3, 128.9, 115.7, 115.5, 81.3, 79.5, 77.3, 77.0, 76.7, 76.6, 48.3, 46.4, 40.4, 40.3, 33.9, 33.8, 31.4, 31.4, 31.3, 31.2, 31.2, 23.8, 23.7, 22.2, 22.2. HRMS (ESI) $[\text{M}+\text{H}]^+$ Anal. Calcd for $\text{C}_{15}\text{H}_{21}\text{FNOS}$: 282.1328; Found: 282.1335.

Table S1: Crystal data and structure refinement for **4c**.

Empirical formula	C ₁₅ H ₁₄ FNOS
Formula weight	275.33
Temperature	293 K
Wavelength	0.71073 Å
Crystal system, space group	Triclinic, <i>P</i> -1
Unit cell dimensions	a = 5.9287 (4) Å, b = 7.3176 (4) Å, c = 16.1549 (12) Å. α = 101.927 (6)°, β = 96.052 (6)°, γ = 90.294 (5)°
Volume	681.65 (8) Å ³
Z, Calculated density	2, 681.65 (8) Mg/m ³
F ₀₀₀	288
Crystal size	0.30 x 0.25 x 0.20 mm
Theta range for data collection	2.6 to 27.5°.
Limiting indices	-7 ≤ h ≤ 6, -9 ≤ k ≤ 8, -20 ≤ l ≤ 20
Reflections collected / unique	5575 / 2265 [R(int) = 0.025]
Refinement method	Full-matrix least-squares on F ²
Data / restraints / parameters	3125 / 0 / 172
Goodness-of-fit on F ²	1.03
Final R indices [I > 2σ(I)]	R1 = 0.0470, wR2 = 0.0991
R indices (all data)	R1 = 0.0668, wR2 = 0.1125
Largest diff. peak and hole	0.20 and -0.21 e.Å ⁻³

Table S2: Bond lengths [Å] and angles [°] for **4c**.

atoms	length	atoms	length
S10—C9	1.6749 (17)	C7—O8—C9	120.89 (14)
F19—C16	1.363 (2)	C9—N11—C12	124.84 (16)
O8—C7	1.449 (3)	C2—C1—C6	120.41 (18)
O8—C9	1.328 (2)	C1—C2—C3	120.2 (2)
N11—C9	1.326 (2)	C2—C3—C4	120.1 (2)
N11—C12)	1.459 (2)	C3—C4—C5	119.4 (2)
C1—C2	1.376 (3)	C4—C5—C6	120.92 (19)
C1—C6	1.384 (3)	C1—C6—C5	119.08 (18)
C2—C3	1.377 (4)	C1—C6—C7	121.10 (17)
C3—C4	1.384 (4)	C5—C6—C7	119.80 (18)
C4—C5	1.382 (3)	O8—C7—C6	108.92 (15)
C5—C6	1.379 (3)	S10—C9—O8	125.28 (12)
C6—C7	1.499 (3)	S10—C9—N11	123.35 (14)
C12—C13	1.510 (2)	O8—C9—N11	111.37 (15)
C13—C18	1.388 (3)	N11—C12—C13	113.03 (14)
C13—C14	1.383 (3)	C14—C13—C18	118.53 (16)
C14—C15	1.374 (3)	C12—C13—C14	119.92 (16)
C15—C16	1.361 (3)	C12—C13—C18	121.55 (17)
C16—C17	1.368 (3)	F19—C16—C17	118.4 (2)
C17—C18	1.377 (3)	F19—C16—C15	118.77 (19)

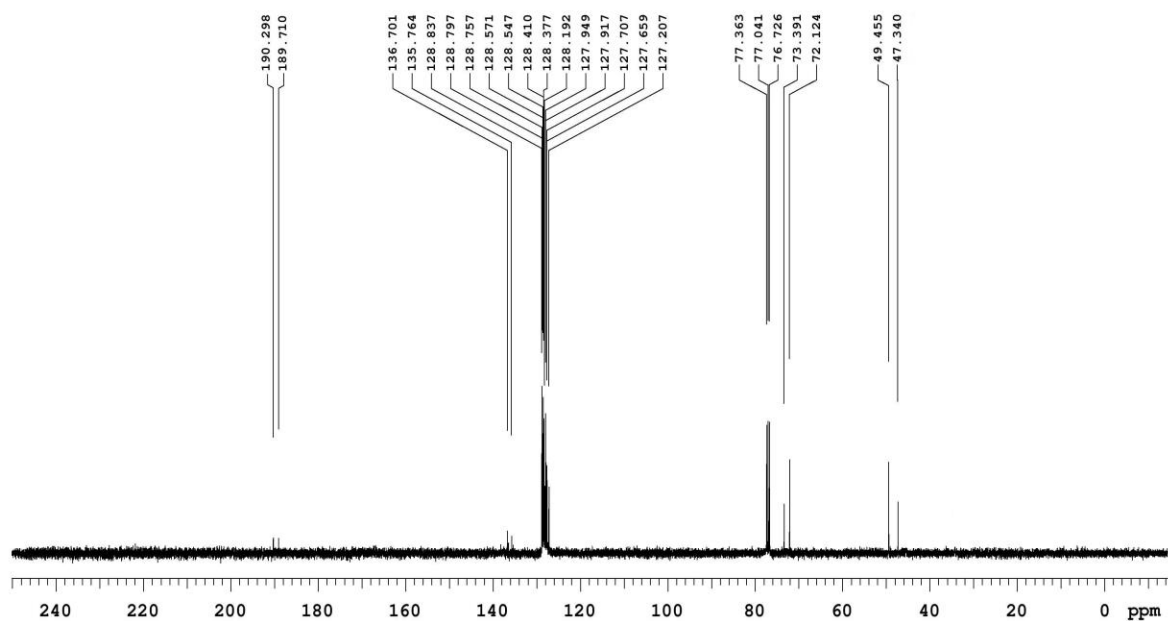
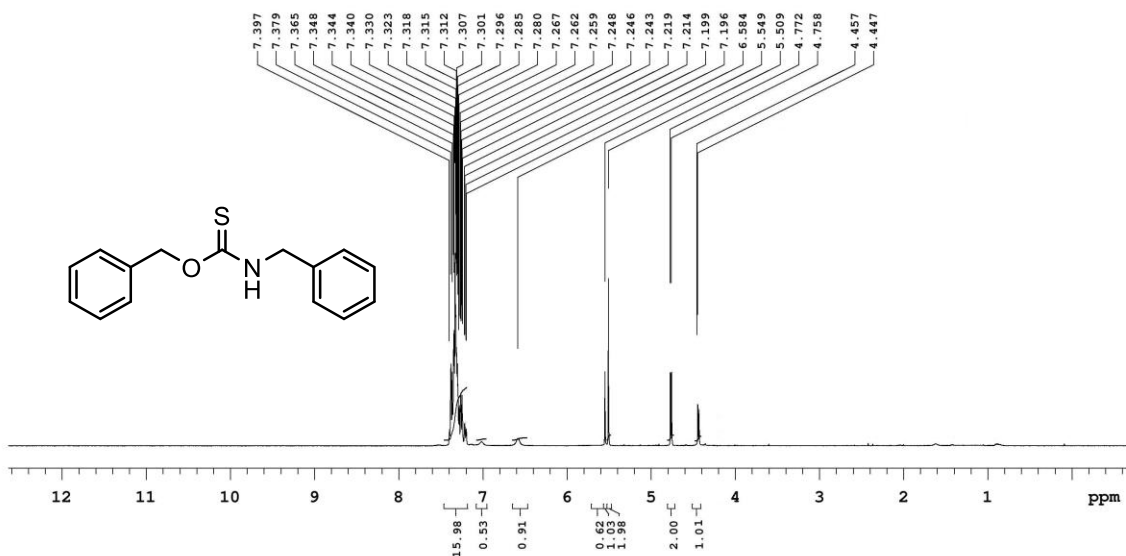


Figure S1: ¹H and ¹³C NMR spectra of 4a.

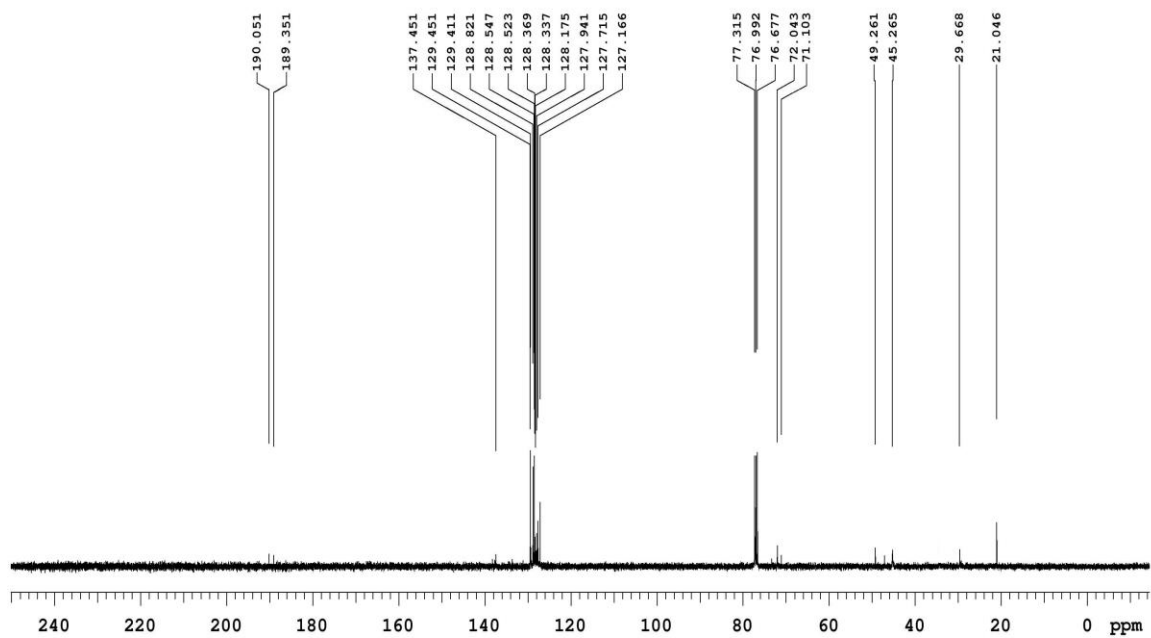
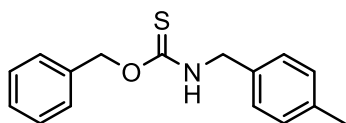
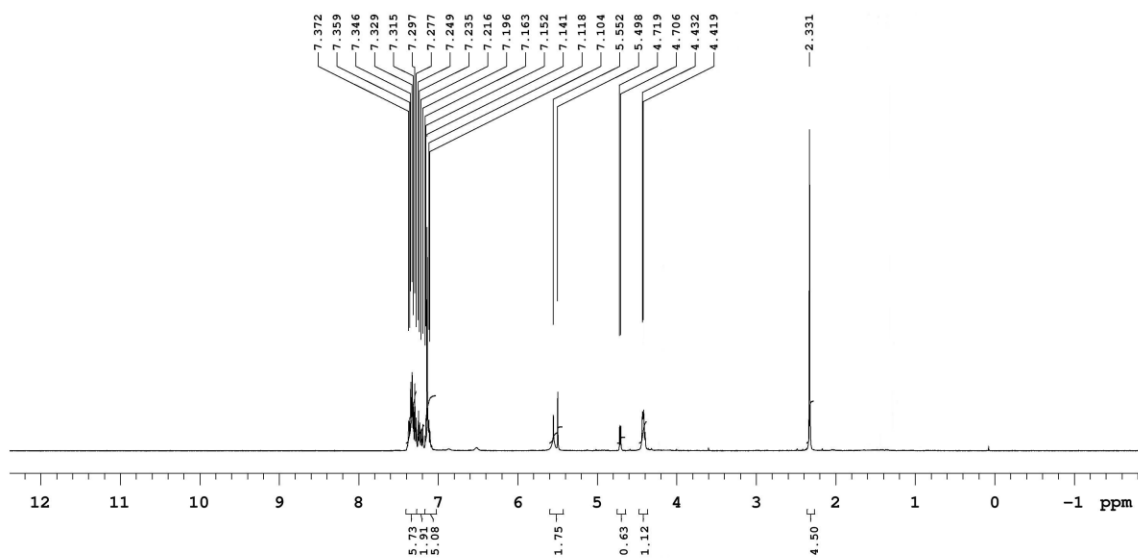


Figure S2: ¹H and ¹³C NMR spectra of 4b.

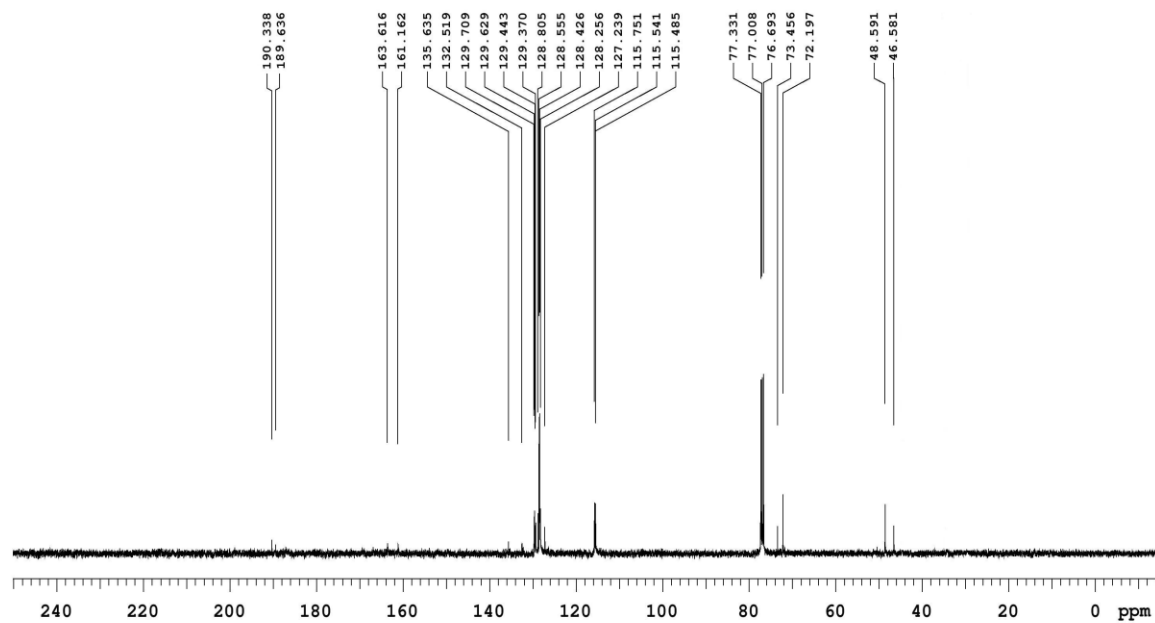
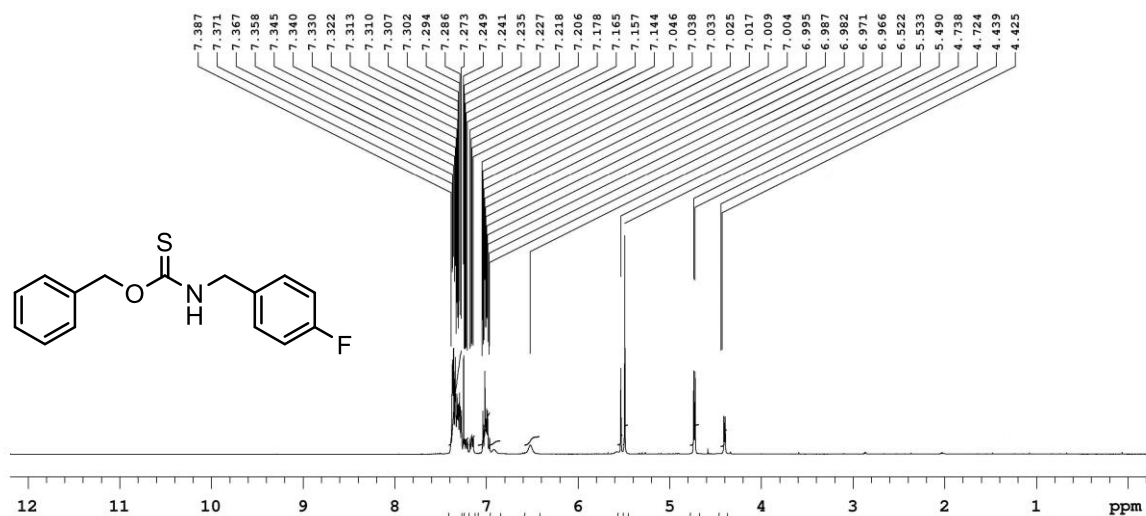


Figure S3: ¹H and ¹³C NMR spectra of 4c.

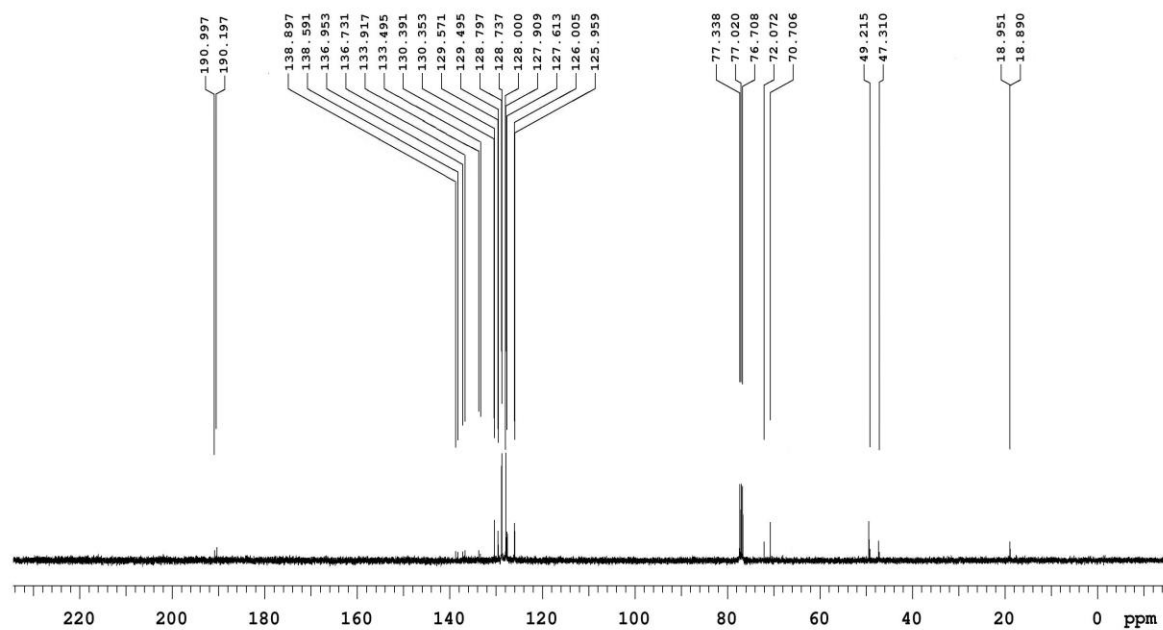
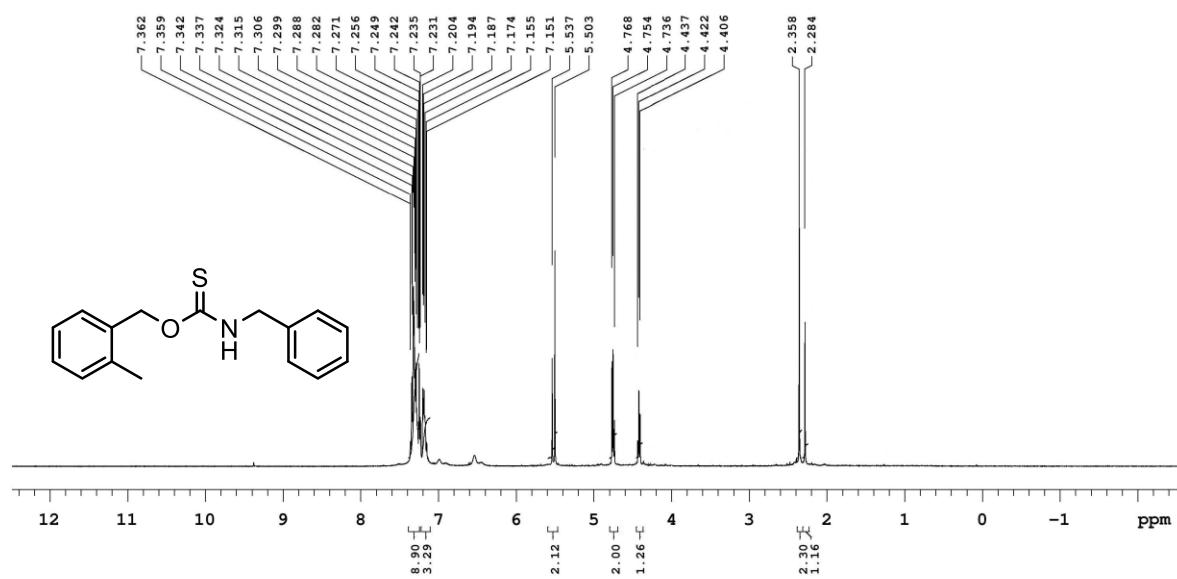


Figure S4: ¹H and ¹³C NMR spectra of 4d.

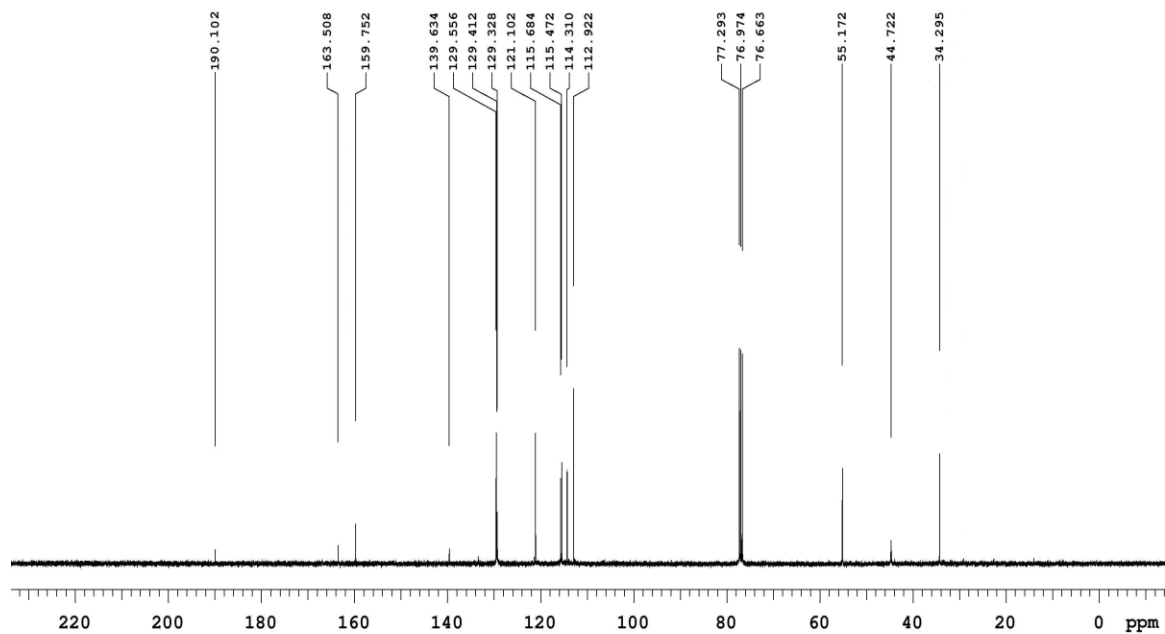
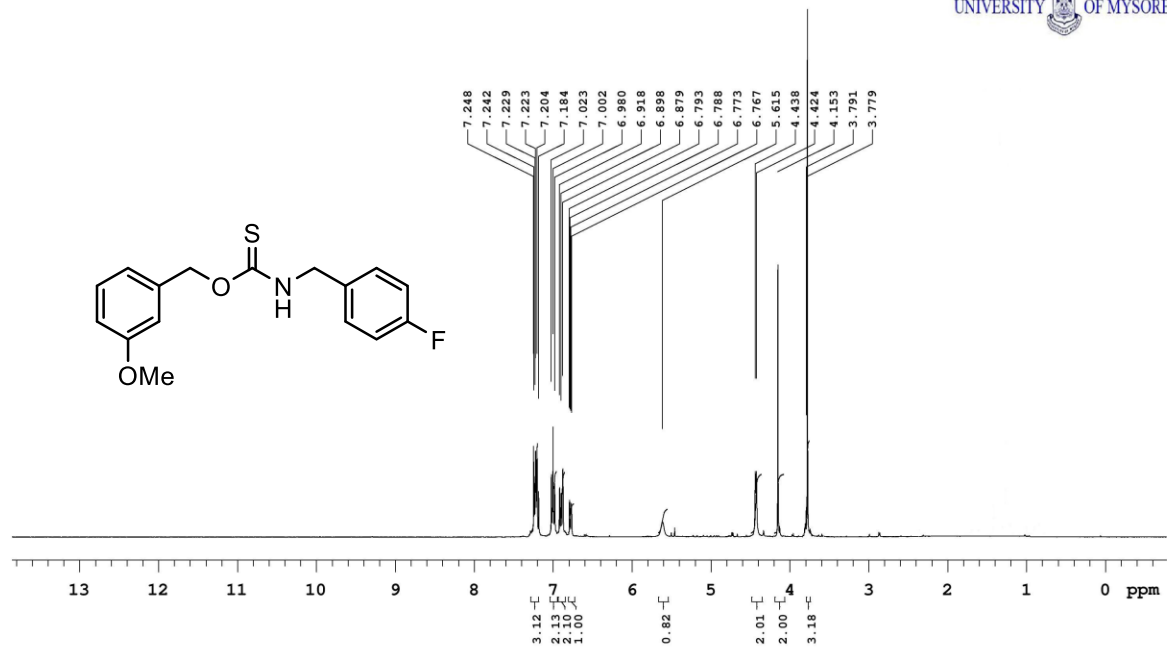


Figure S5: ¹H and ¹³C NMR spectra of 4e.

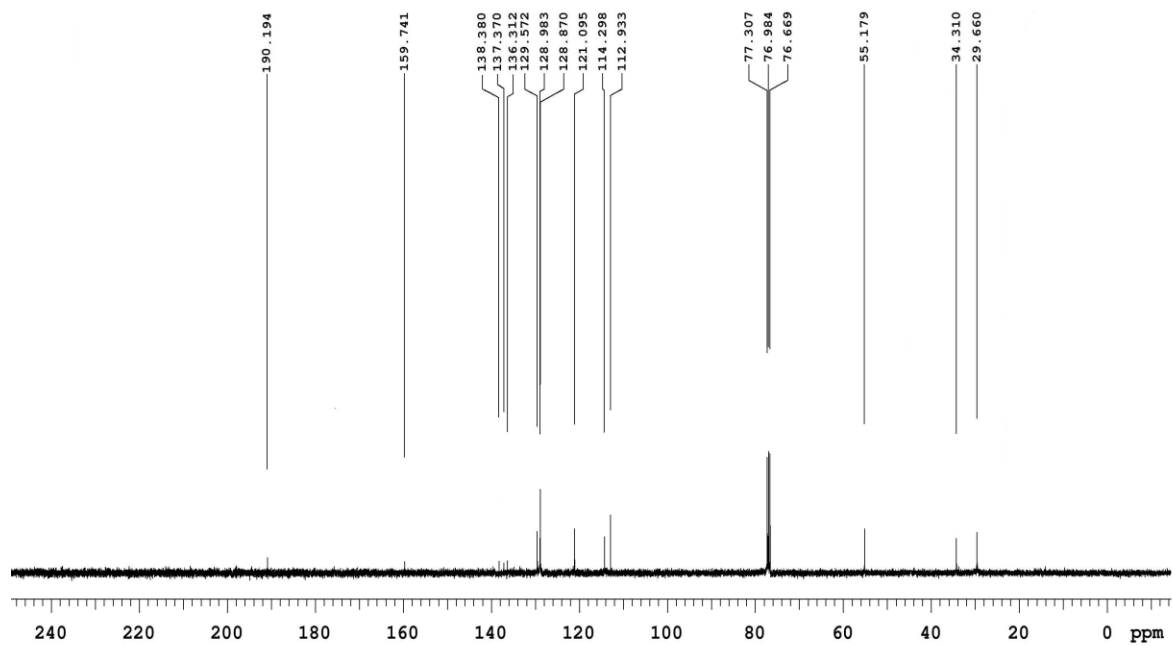
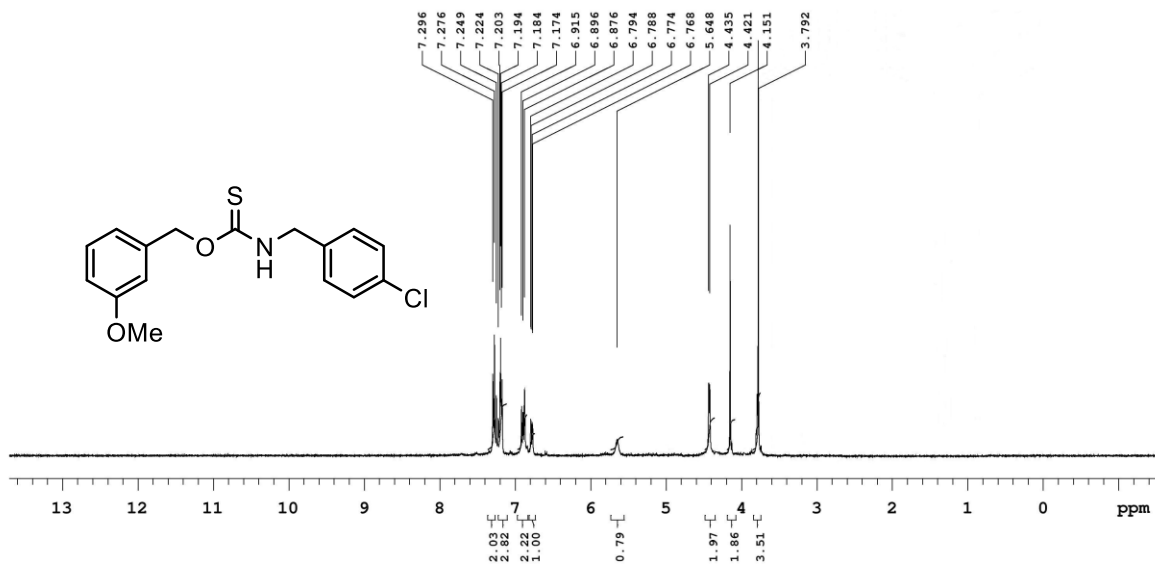


Figure S6: ¹H and ¹³C NMR spectra of 4f.

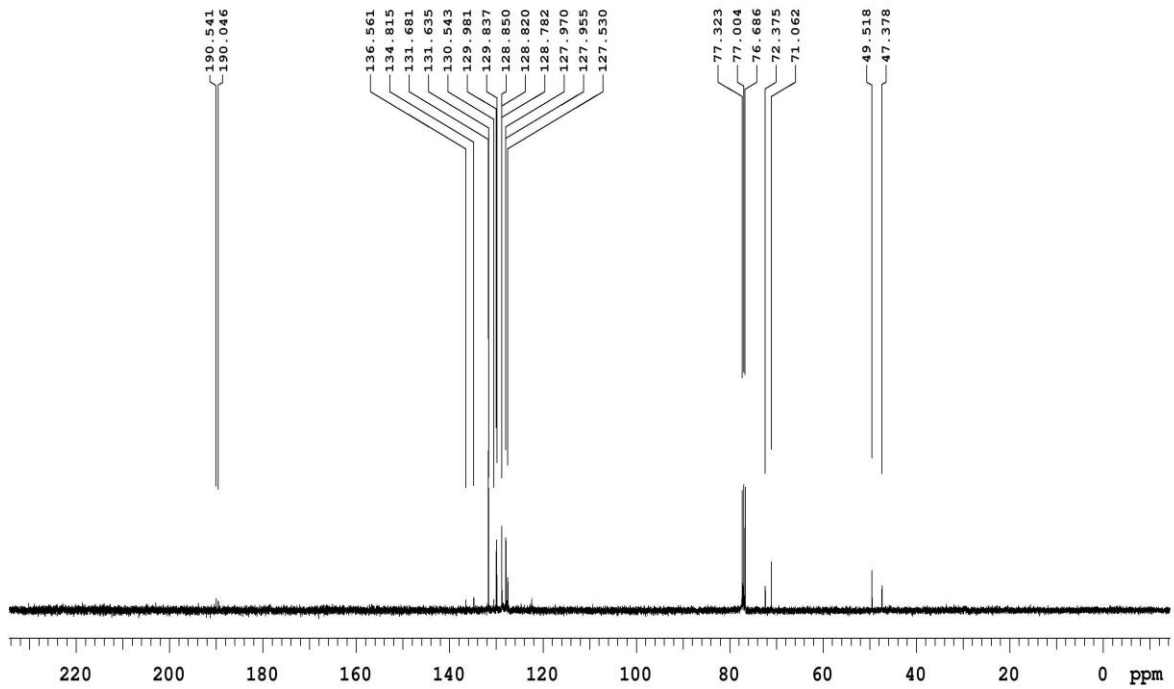
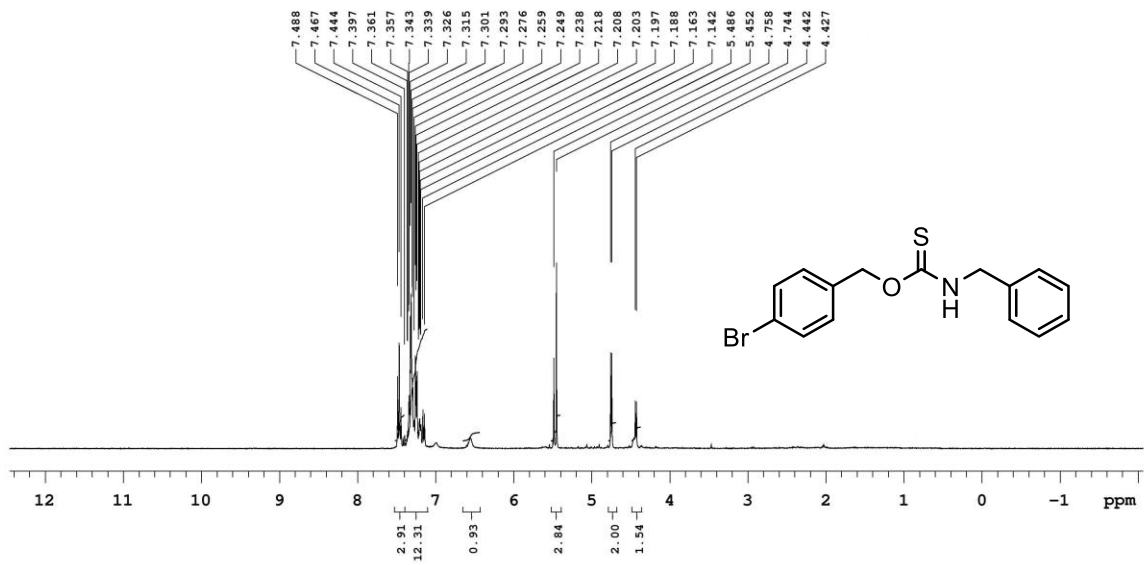


Figure S7: ^1H and ^{13}C NMR spectra of **4g**.

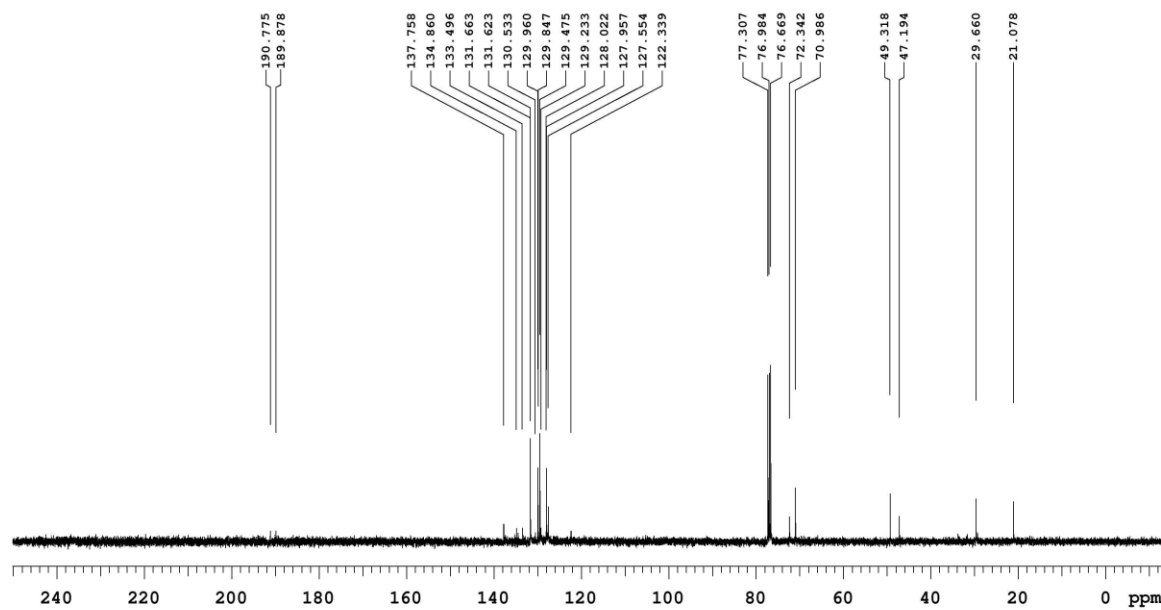
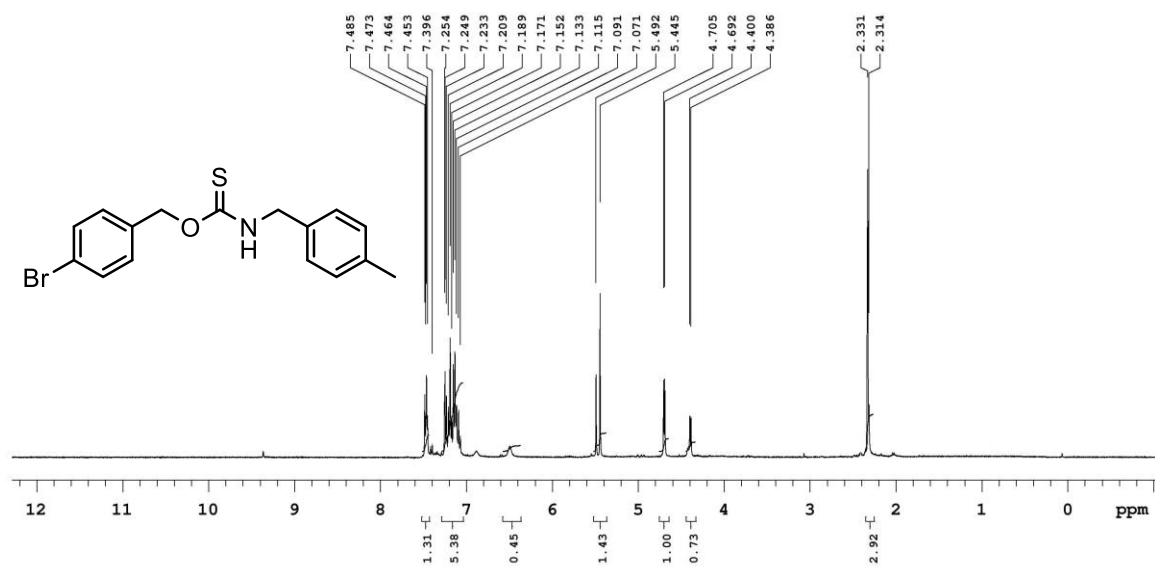


Figure S8: ¹H and ¹³C NMR spectra of 4h.

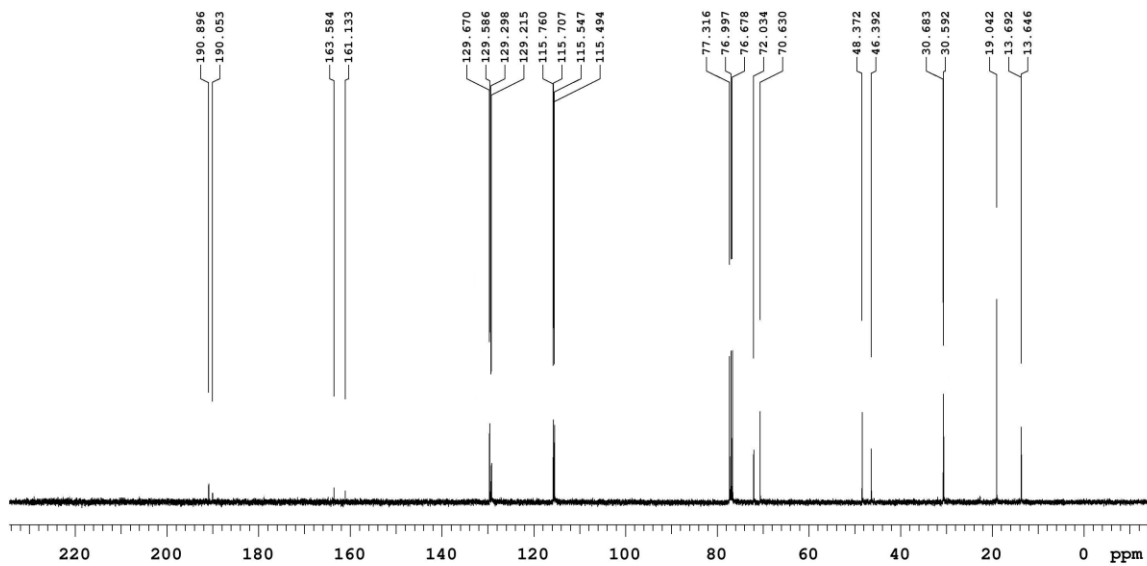
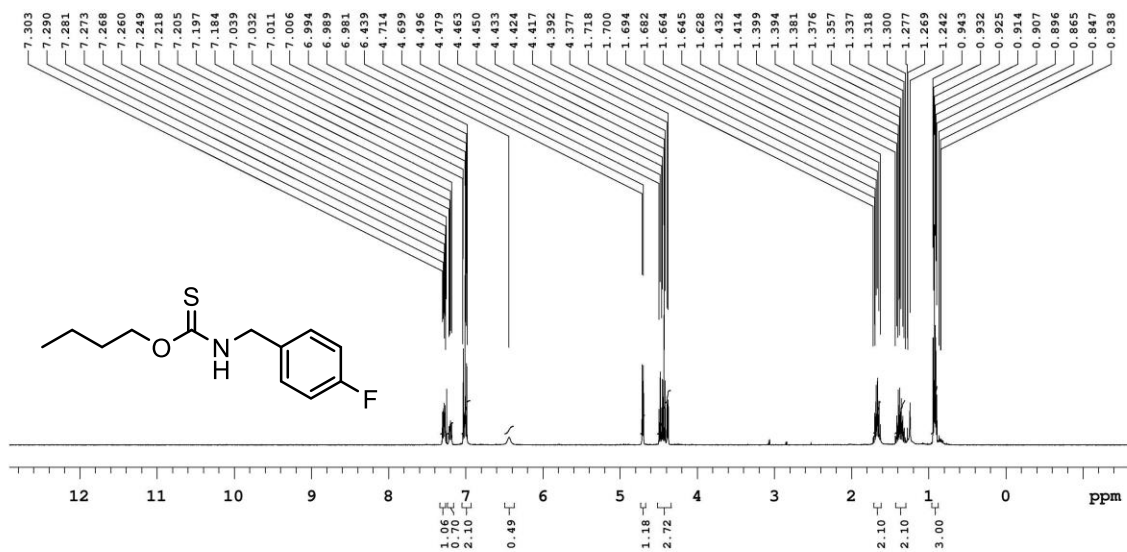


Figure S9: ^1H and ^{13}C NMR spectra of 4i.

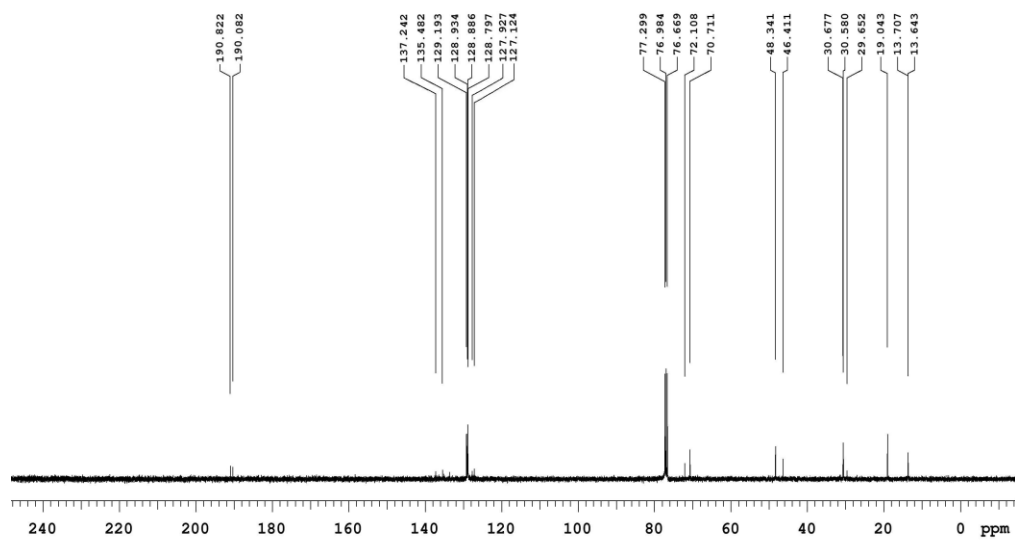
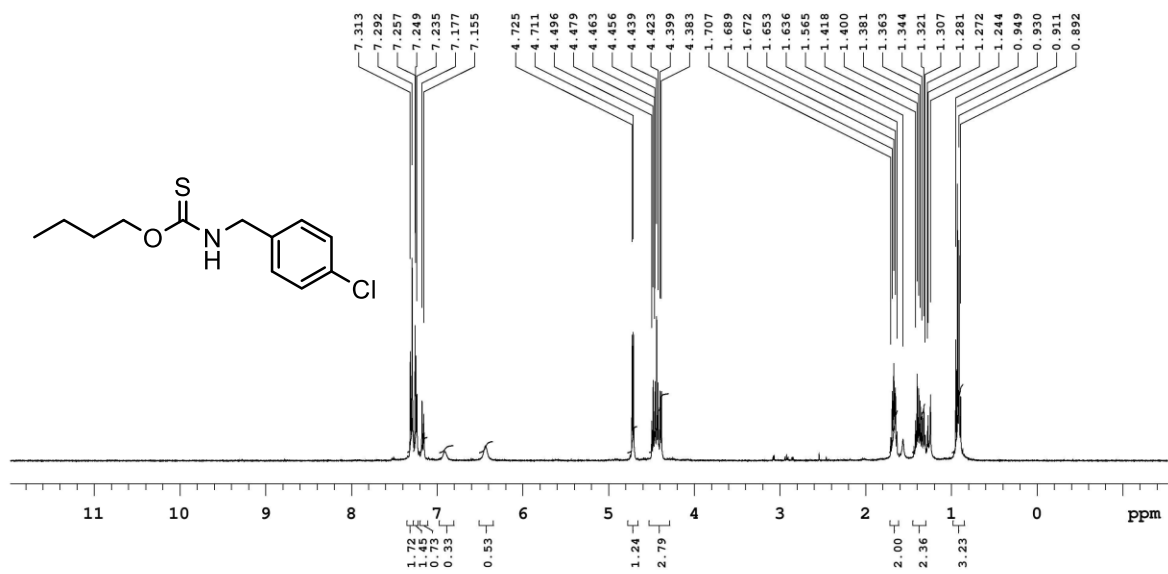


Figure S10: ¹H and ¹³C NMR spectra of 4j.

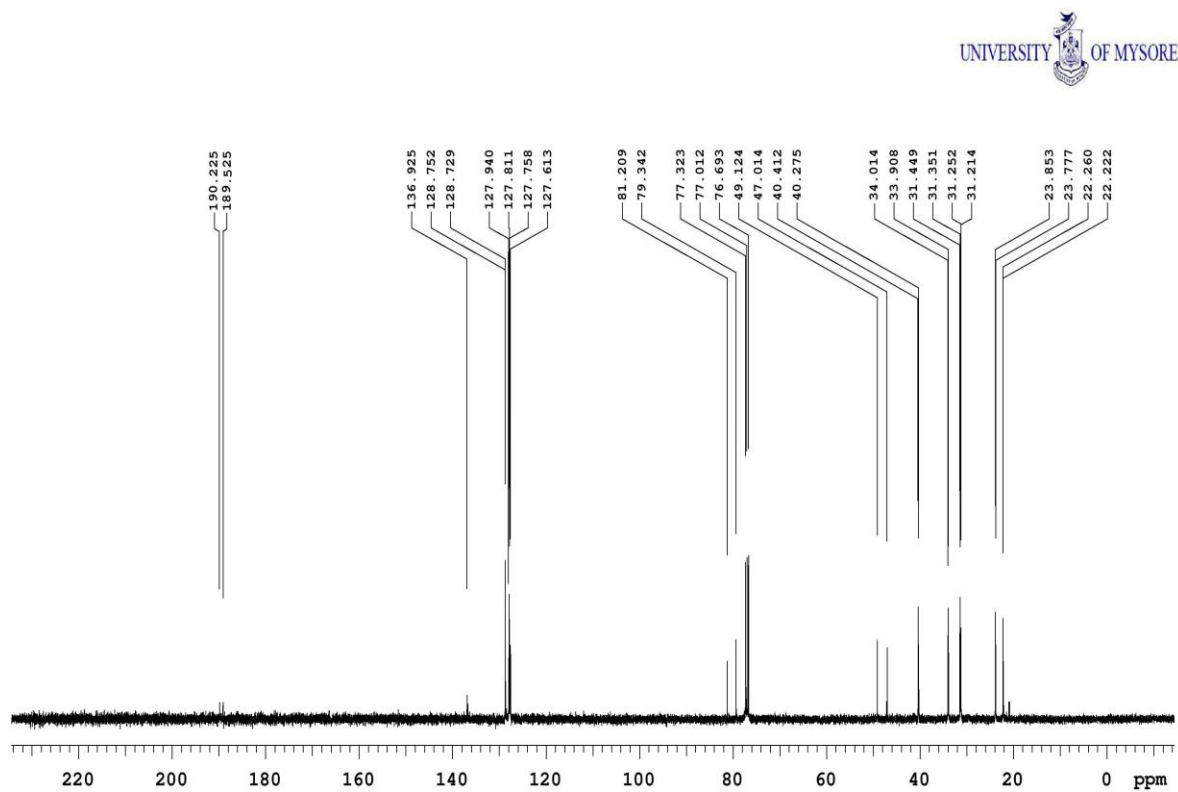
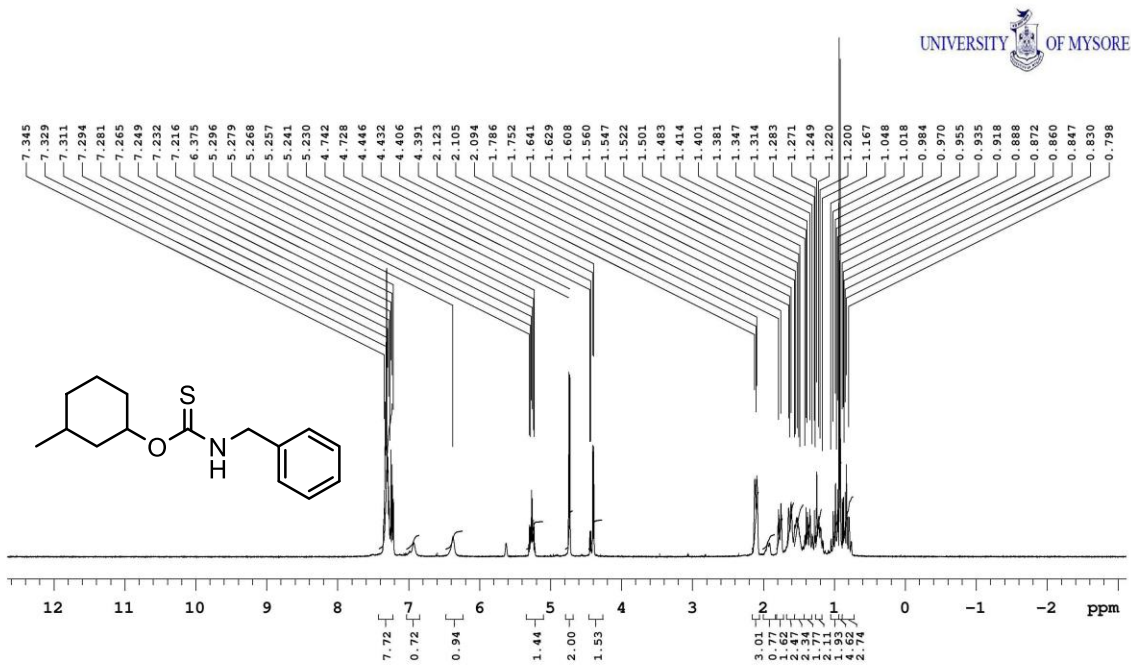


Figure S11: ^1H and ^{13}C NMR spectra of 4k.

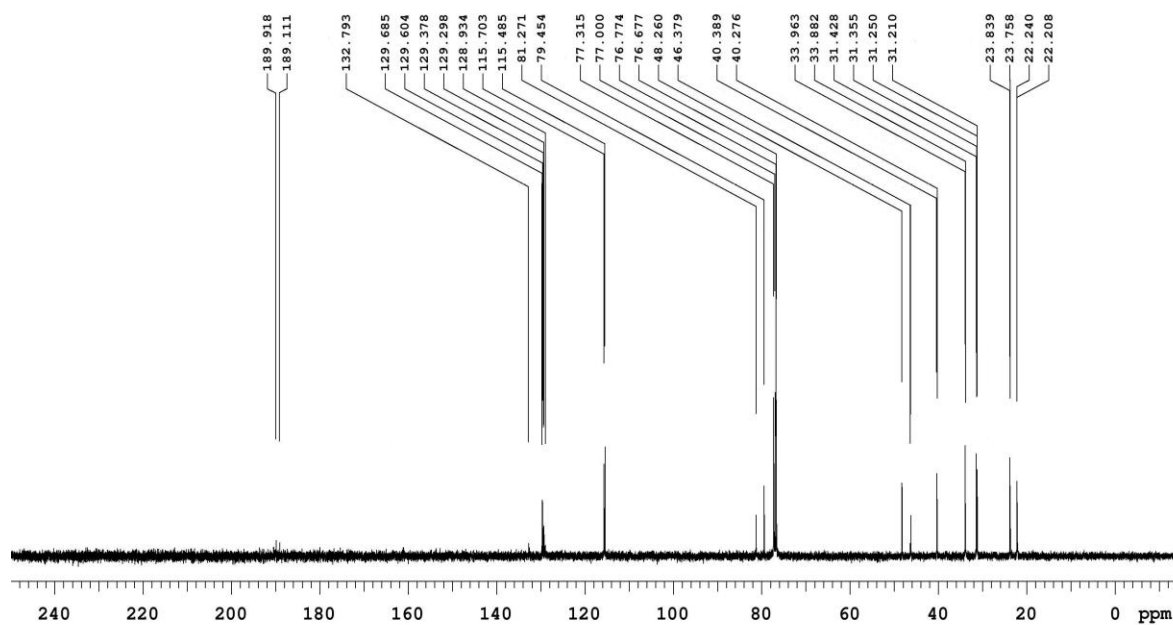
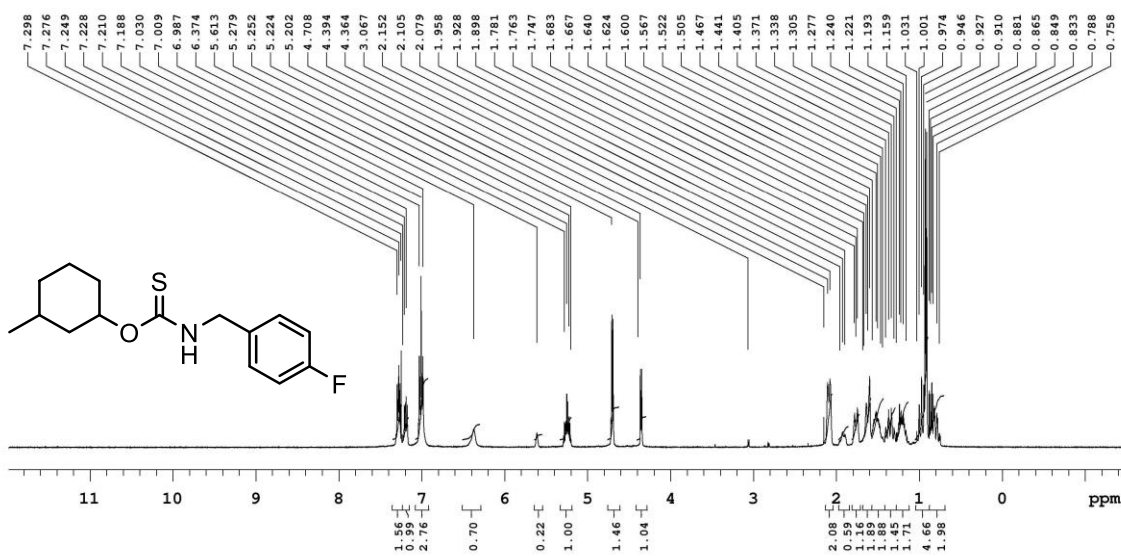
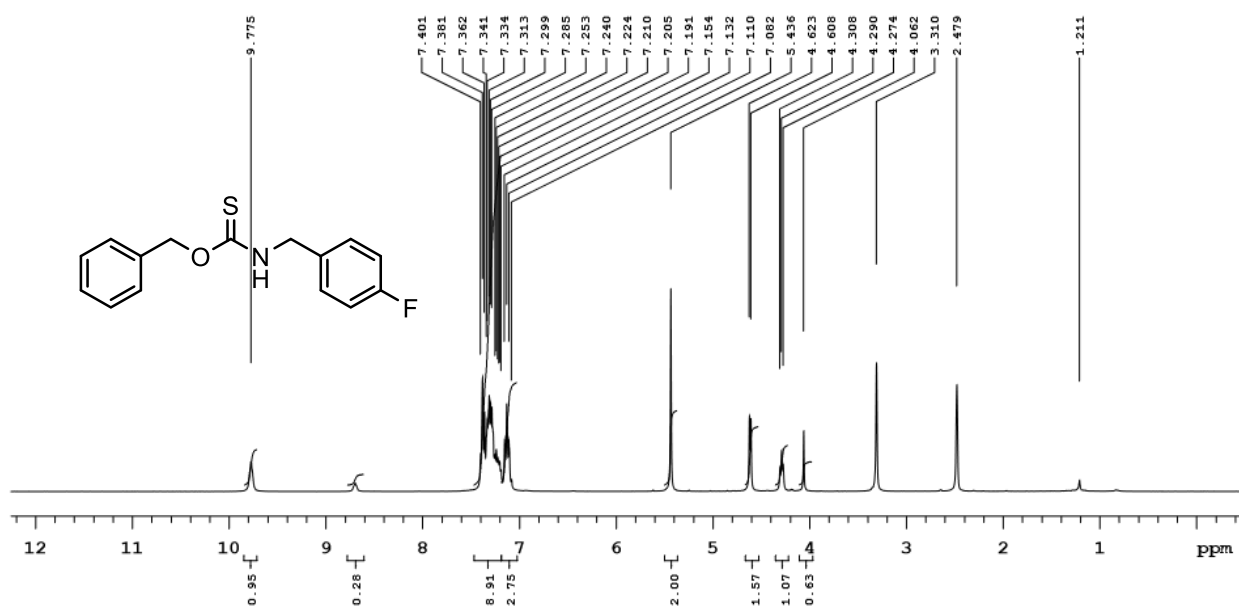


Figure S12: ¹H and ¹³C NMR spectra of 41.



¹H NMR spectrum of **4c** in DMSO-*d*₆ under normal conditions.

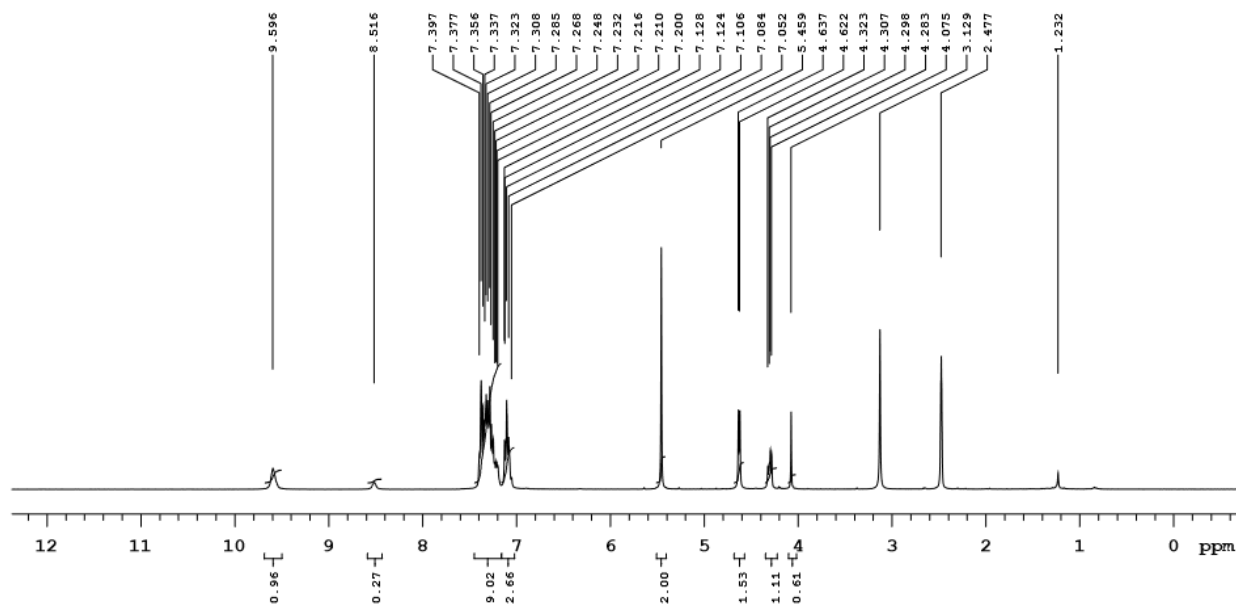


Figure S13: ¹H spectrum of **4c** in DMSO-*d*₆ after heating to 60 °C.

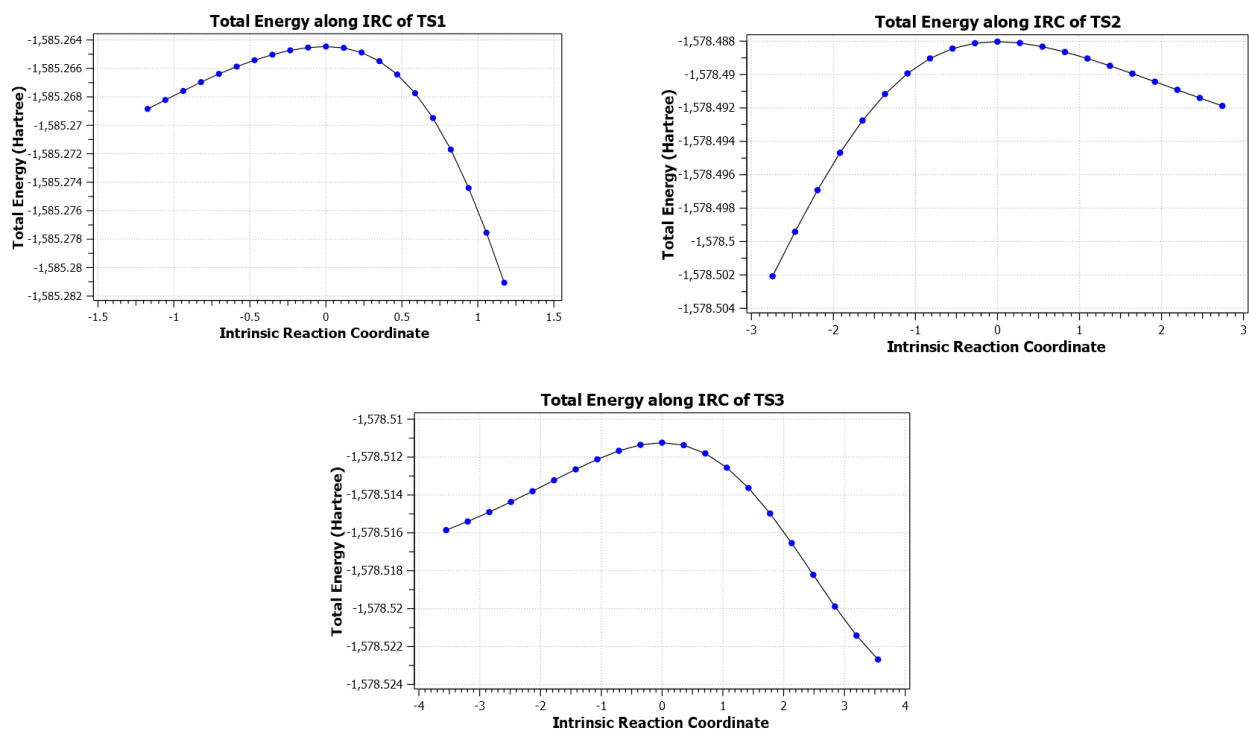
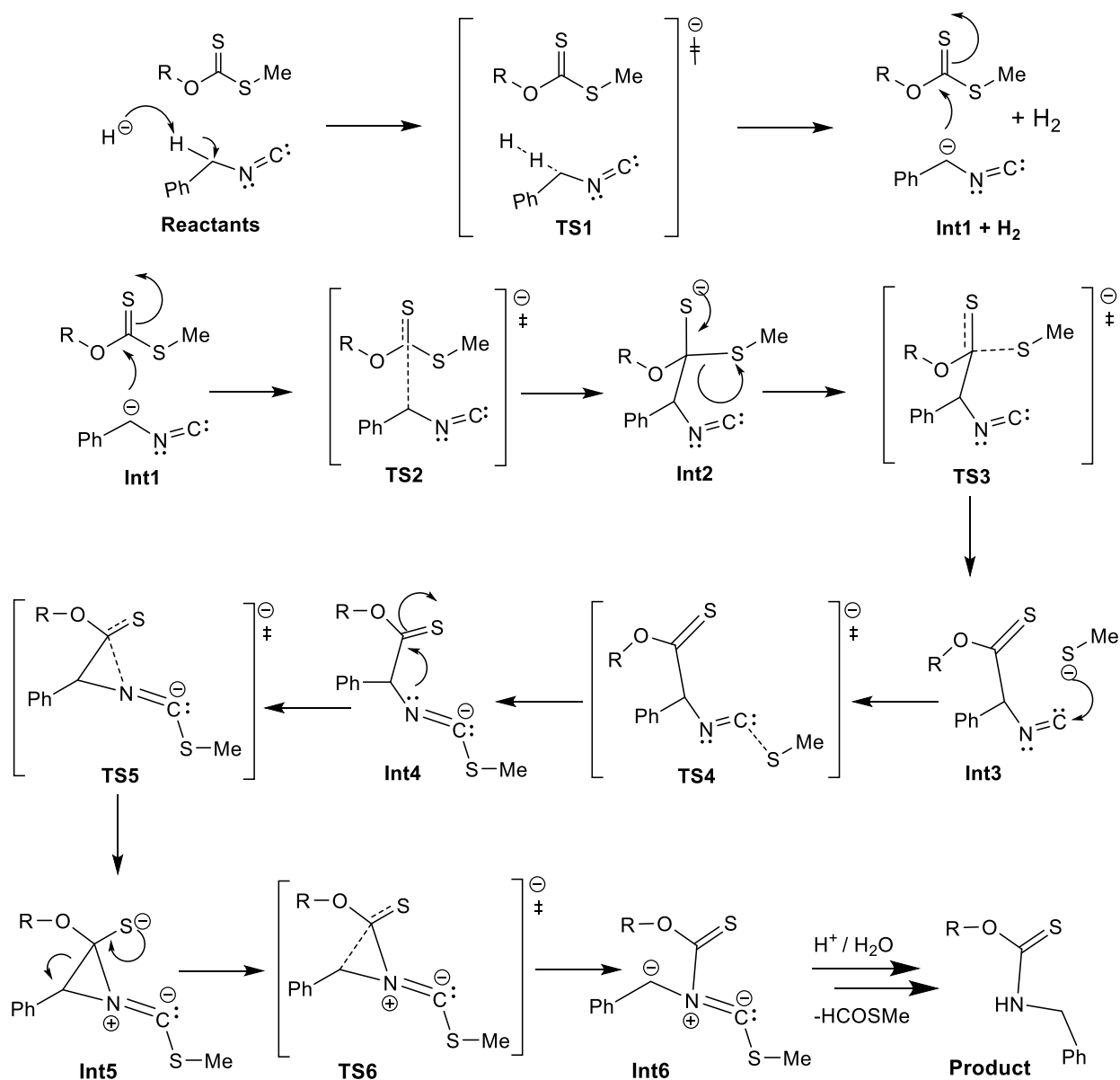


Figure S14: Total energies (Hartrees) along the intrinsic reaction coordinates (IRC) calculated at the HF/6-31G(d) level of theory in the gas phase for the two transition states of the proposed mechanism (see Scheme 2, Figures 4 and 5 in the main text).

Table S3: Relative electronic energies (E_{ele}), activation energies (E_{thermal}), enthalpies (H), free energies (G) in kJ mol^{-1} calculated at the B3LYP/6-311++G(d,p) level of theory in DMF solvent system for the species involved in the proposed mechanism.

Species	E_{ele}	E_{thermal}	H	G
Reactants	0.0	0.0	0.0	0.0
TS1	45.2	42.2	42.2	57.9
Int1	-43.2	-29.8	-29.8	-7.7
TS2	-5.4	5.3	5.3	44.5
Int2	-65.0	-46.1	-46.1	-3.4
TS3	-37.6	-21.4	-21.4	16.7
Int3	-63.1	-44.7	-44.7	-22.0



Scheme S1: The alternative mechanism previously considered [Reference S14], involving the initial nucleophilic addition of a preformed benzylic α -carbanion to the thiocarbonyl group of the xanthate.

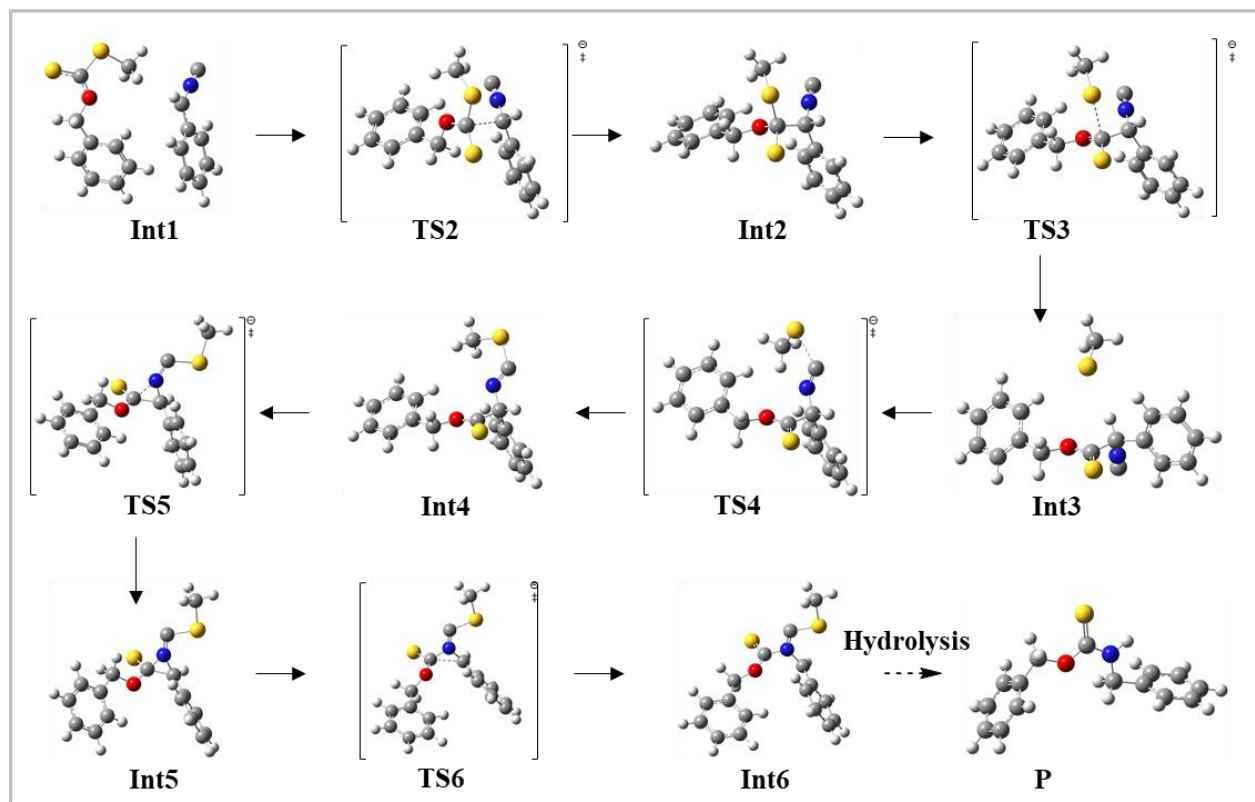
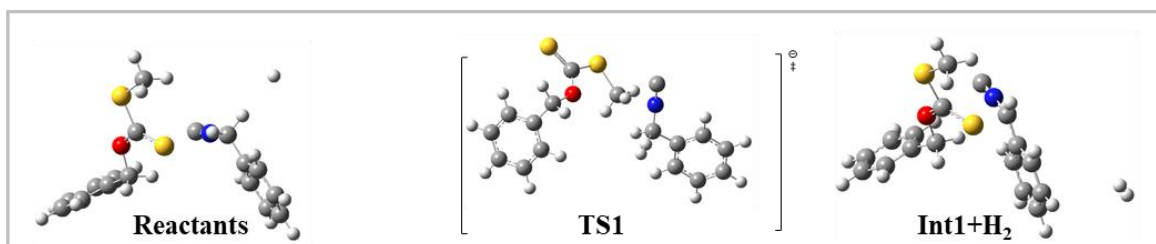


Figure S15: The optimized geometries of reactants, transition states, intermediates, and the product of the proposed reaction mechanism at the HF/6-31G(d) level of theory in gas phase (note: the reaction leading to the proton abstraction from the benzylic CH₂ group to form the Intermediate **Int1** via the transition state **TS1** is shown on the first line. For the subsequent steps, i.e., **Int1–Int6**, the geometry optimizations were performed without including the H₂. However, the energy of the H₂ has been added to the energy of each species shown in Figure S16 to correctly compare the relative energies for both proposed mechanisms).

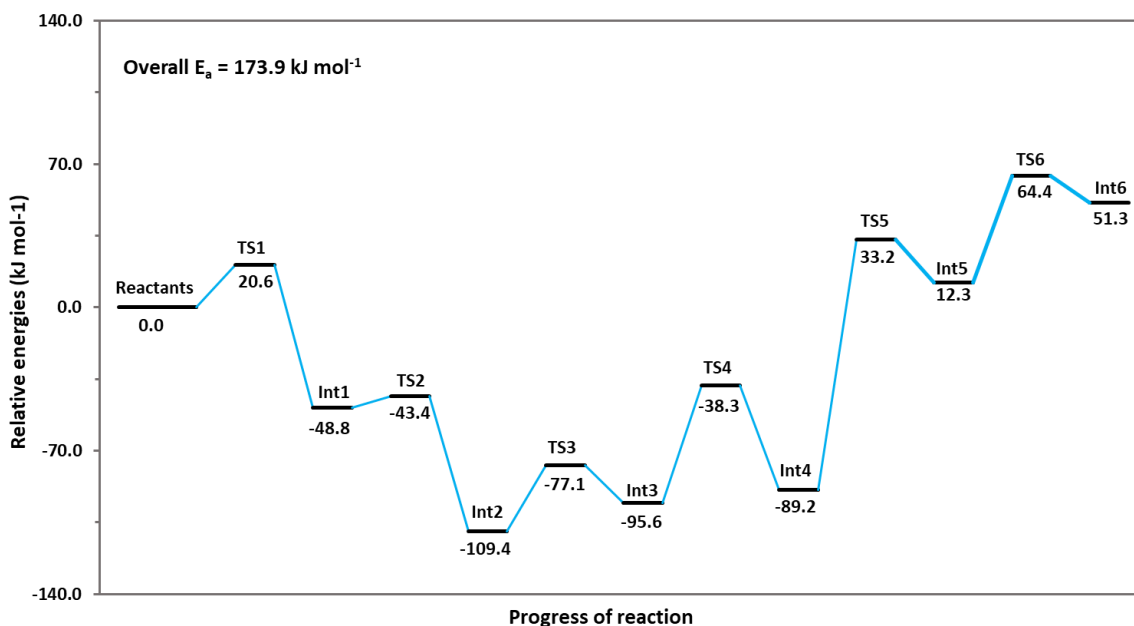


Figure S16: Relative energies of reactants, transition states (TS1–TS6), and intermediates (Int1–Int5) of the previously proposed reaction mechanism [Reference SI4] computed (this work) at the B3LYP/6-311++G(d,p) level of theory in a DMF solvent system.

References

- [SI1] Bruker, APEX2 and SAINT. Bruker AXS Inc, Madison, Wisconsin, USA 2009.
- [SI2] (a) Sheldrick, G. M. *Acta. Cryst.* **2008**, A64, 112-122. (b) Sheldrick, G. M. *ActaCryst.* **2015**, C71, 3-8.
- [SI3] *Gaussian 09*, Revision C.01, Frisch, M. J.; Trucks, G. W.; Schlegel, H. B.; Scuseria, G. E.; Robb, M. A.; Cheeseman, J. R.; Scalmani, G.; Barone, V.; Mennucci, B.; Petersson, G. A.; Nakatsuji, H.; Caricato, M.; Li, X.; Hratchian, H. P.; Izmaylov, A. F.; Bloino, J.; Zheng, G.; Sonnenberg, J. L.; Hada, M.; Ehara, M.; Toyota, K.; Fukuda, R.; Hasegawa, J.; Ishida, M.; Nakajima, T.; Honda, Y.; Kitao O.; Nakai, H.; Vreven, T.; Montgomery Jr. J. A.; Peralta, J. E.; Ogliaro, F.; Bearpark, M.; Heyd, J. J.; Brothers, E.; Kudin, K. N.; Staroverov, V. N.; Kobayashi, R.; Normand, J.; Raghavachari, K.; Rendell, A.; Burant, J. C.; Iyengar, S. S.; Tomasi, J.; Cossi, M.; Rega, N.; Millam, J. M.; Klene, M.; Knox, J. E.; Cross, J. B.; Bakken, V.; Adamo, C.; Jaramillo, J.; Gomperts, R.; Stratmann, R. E.; Yazyev, O.; Austin, A. J.; Cammi, R.; Pomelli, C.; Ochterski, J. W.; Martin, R. L.; Morokuma, K.; Zakrzewski, V. G.; Voth, G. A.; Salvador, P.; Dannenberg, J. J.; Dapprich, S.; Daniels, A. D.; Farkas, Ö.; Foresman, J. B.; Ortiz, J. V.; Cioslowski, J.; Fox, D. J. *Gaussian*, Inc., Wallingford CT, 2009.
- [SI4] *Beilstein Arch.* **2019**, 201926. doi:10.3762/bxiv.2019.26.v1]